JurnalPolimesin
Department of Mechanical Engineering
State Polytechnic of Lhokseumawe
http://e-jurnal.pnl.ac.id/polimesin
e-ISSN : 2549-1999 No. : 2 Month : April
p-ISSN : 1693-5462 Volume : 22 Year : 2024

Article Processing Dates: Received on 2024-01-30, Reviewed on 2024-02-12, Revised on 2024-02-21, Accepted on 2024-03-29 and Available online on 2024-04-30

Effect of heat input on the microstructure and hardness of AISI 321 stainless steel welds using ER 347 filler metal

Herry Oktadinata[1*], Dewin Purnama[2], Debby Laksana Anugrah[1]
[1]Mechanical Engineering, Universitas Jenderal Achmad Yani, Cimahi, 40513, Indonesia
[2]Mechanical Engineering, Politeknik Negeri Jakarta, Depok, 16425, Indonesia
*Corresponding author: herry.oktadinata@yahoo.com

Abstract
Stainless steel is widely used in various fields, one of which is AISI 321, which is used for high-temperature applications because of its high resistance to creep and intergranular corrosion. The type of filler metal and heat input on stainless steel welds play an essential role in determining the microstructure and mechanical properties of the welded joints. The purpose of this experiment was to evaluate the microstructure and mechanical properties of AISI 321 stainless steel welds with variations in heat input. This study is expected to explore the performance of this weld joint, which can be anticipated in relevant fields. The welding method used in this experiment was Gas Tungsten Arc Welding (GTAW) with ER 347 as filler metal. Welding was carried out on three samples with a heat input of 0.92 kJ/mm, 0.64 kJ/mm, and 0.52 kJ/mm, respectively. The tests included tensile strength, Vickers microhardness, and microstructure observations. The tensile test results showed that a fracture occurred in the Base Metal (BM) area, indicating that the strength of the weld joint was higher than that in the BM. The Vickers microhardness test results showed that the Weld Metal's hardness (WM) was the highest, followed by the Heat-Affected Zone (HAZ) and BM. The welding experiment that used three variations in heat input demonstrated that higher heat input lowered the hardness of the weld joint. The microstructure observation results around the fusion line demonstrated the presence of step and ditch structures. The ditch structure indicates intergranular corrosion.

Keywords:
AISI 321, GTAW, microstructure, hardness, heat input.

1 Introduction

Stainless steel, widely used in various fields such as oil and gas, food industry, medical, and so on, is a corrosion-resistant material. Although stainless steel consists of several types (austenitic, ferritic, duplex, and martensitic), austenitic stainless steel is the most commonly used. This is because, in addition to being able to be used over a wide temperature range from low to high, austenitic stainless steel also has high impact toughness and good weldability.

It is widely known that austenitic stainless steel is susceptible to sensitization when exposed at elevated temperatures ranging from 500°C to 800°C. This phenomenon is characterised by the formation of chromium carbide precipitates at the grain boundaries. Consequently, a chromium-depleted zone is formed in the grain boundaries, leading to a decrease in corrosion resistance. Therefore, this steel is susceptible to intergranular corrosion under certain conditions, such as high-temperature usage or as a result of welding processes [1]–[6].

The Heat-Affected Zone (HAZ) in austenitic stainless steel is vulnerable to intergranular corrosion, known as weld decay. Within the sensitization temperature range (500°C to 800°C), carbon atoms rapidly migrate to the grain boundaries and consolidate with chromium to form chromium carbides. Weld decay issues can be avoided through several methods: (1) solution treatment, which involves applying heat treatment after welding, followed by rapid cooling, (2) using low-carbon stainless steel (such as "L" type), or (3) using stainless steel that contains titanium (Ti) or niobium (Nb), such as AISI 321 or AISI 347 [4]. Previous work on dissimilar joints of SS 321 and SS 347 found that the welded joint with ER 347 filler metal exhibited improved tensile strength and hardness compared to the joint made by ER 321 filler metal [7]. Using filler metal type 347 which contained Nb provided better sensitization performance compared to 316 in AISI 316 austenitic stainless steel weld joints [8].

Austenitic stainless steel type AISI 321 is commonly used for high-temperature applications due to its high resistance to creep and intergranular corrosion. AISI 321 is nearly identical to AISI 304, with the only difference being the addition of titanium (Ti) to stay away from intergranular corrosion during high-temperature usage or welding. In the high temperature applications, the presence of titanium in AISI 321 mitigates intergranular corrosion by forming the precipitation of titanium carbides, thus limiting the development of chromium-rich carbides [9]–[11]. When exposed to high temperatures for extended periods of time, this makes AISI 321 more resistant to intergranular corrosion.

The type of filler metal and heat input in welding stainless steel plays a crucial role in deciding the microstructure and mechanical properties in the weld metal [12]–[15]. The filler metal type contributes to the resulting chemical composition in the fusion zone, ultimately affecting the microstructure that forms. On the other hand, the heat input value affects the cooling rate. A higher heat input slows down the cooling rate and vice versa. The cooling rate will impact the hardness value. Welding with low heat input results in higher microhardness and tensile strength because of the higher retained austenite content compared to high heat input [16], [17]. Increasing the heat input also widens the Heat-Affected Zone (HAZ) [16], [18], [19].

The higher the heat input, the longer is the retention time within the sensitisation temperature range, which allows the formation of chromium carbide precipitates [4], [20]. High heat input in welding can increase the tendency for the formation of larger carbides compared to low heat input welding [21], [22].

Filler metal type 347 containing Nb is known to provide better sensitization performance during welding operations. However, an experiment using this filler type is required to study the relationship between the heat input parameter and microstructure of the weld metal, which affects its hardness. The objective of this experiment was to assess the microstructure and hardness of the welded joints of AISI 321 steel using ER 347 filler metal with varying heat inputs. This study is expected to explore the performance of this weld joint, which can be anticipated in the relevant field. The testing conducted includes tensile strength, microhardness, and microstructure observations. Microstructure observations are performed around the welded joint.

2 Research Methods

AISI 321 stainless steel was used as the base metal. ER 347 filler metal with a diameter of 1.6 mm was used. The chemical compositions of the AISI 321 steel and ER 347 filler metal are listed in Table 1, while their mechanical properties are listed in Table 2. The data for the chemical composition and mechanical properties of the filler metal were obtained from the manufacturer's material certificate.

Table 1. Chemical composition of AISI 321 steel and ER 347 filler metal

Material	Weight of elements (%)										
	C	Mn	P	S	Si	Ni	Cr	Mo	Ti	Nb	Cu
AISI 321	0.01	1.81	0.026	0.0001	0.5	9.1	17.26	0.41	0.17	-	0.38
ER 347	0.04	1.3	0.025	0.015	0.4	9.5	19.5	0.3	-	0.4	0.1

Table 2. Mechanical characteristics of AISI 321 steel and ER 347 filler metal

Material	TS (psi)	YS (psi)	Elongation(%)
AISI 321	83500	35700	65
ER 347	88000	58000	42

The welded samples were created by joining two plates with a 60° bevel angle and dimensions of 125 mm × 130 mm × 2 mm (see Fig. 1). The experiment was conducted on three samples using single-pass welding with three heat-input variations. The three samples were named HI, MI, and LI, corresponding to high heat input (0.92 kJ/mm), medium heat input (0.64 kJ/mm), and low heat input (0.52 kJ/mm), respectively.

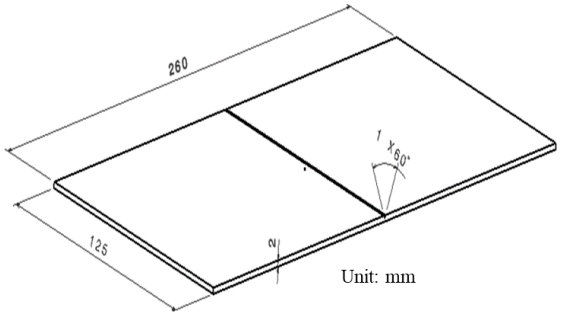

Fig. 1. Material outline.

Using the Gas Tungsten Arc Welding (GTAW) technique and DCEN polarity, each of the three samples was welded together. A ceriated tungsten electrode (EWCe-2) was used in this experiment. Argon shielding gas and gas flow rate of 8 L/min were applied in the 1G (flat) welding position for this experiment. Fig. 2 shows the welded sample results.

Table 3 displays the recorded and presented welding parameters. Heat input E (J/mm) was determined using the Eq. 1.

$$E = U \times I \times 60/v \quad (1)$$

where U = welding voltage (Volt), I = welding current (Ampere), and v = travel speed (mm/min).

Table 3. Welding parameters

Sample code	Voltage (V)	Current (A)	Travel speed (mm/min)	Heat input (kJ/mm)
HI	10.5	50	34	0.92
MI	10.7	70	70	0.64
LI	11	85	107	0.52

Microstructure observation, tensile testing, and Vickers microhardness measurements were conducted on the weld joint region. In each HI, MI, and LI sample, the metallographic specimens were cut perpendicular to the welding direction. A Struers LaboForce-50 grinding and polishing machine was used to grind and polish the mounted specimens. The specimens were ground using silicon carbide abrasive papers with grits of 80 to 2000 and polished using a polishing cloth. Subsequently, the samples were etched with an aqua regia solution with a mixture of 20 ml of HNO_3 and 60 ml of HCl for microstructure feature observation purposes.

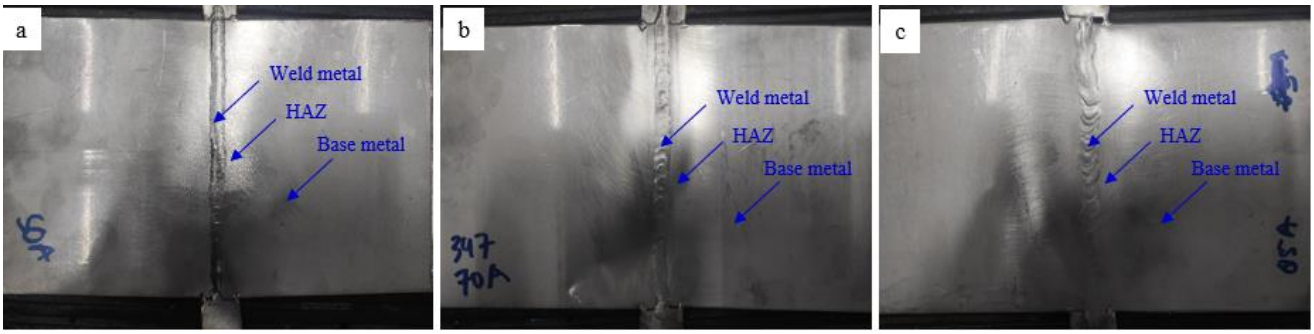

Fig. 2. Welded specimens: a) high heat input (HI), b) medium heat input (MI), and c) low heat input (LI).

Metallographic specimens were observed under an optical microscope, and micrographs were captured. The microscopic examination was performed using a Nikon Eclipse LV 150 optical microscope. Microstructure examination was conducted on the cross-sections of the Base Metal (BM), Heat-Affected Zone (HAZ), fusion boundary, and fusion zone. The observations included the grain growth and the presence of chromium carbide precipitates at the grain boundaries.

Standard specimens for tensile and hardness tests were constructed to determine their mechanical characteristics. Tensile strength measurement was carried out at room temperature utilizing an Instron 5982 universal testing machine with a load capability of 100 kN. Tensile test specimens were prepared according to the ASTM E8 standard, as shown in Fig. 3. Micro Vickers hardness testing was conducted on the weld section using a Zwick Roell microhardness testing machine. In each specimen, Vickers microhardness was estimated in the WM, HAZ, and BM regions. The microhardness test utilized a 300-gram load and was held for 10 s for each measurement (Fig. 4).

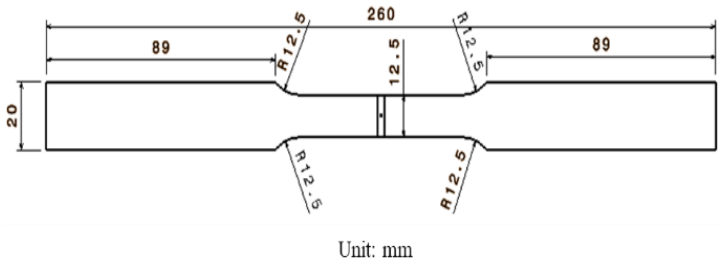

Fig. 3. Tensile test specimen dimensions.

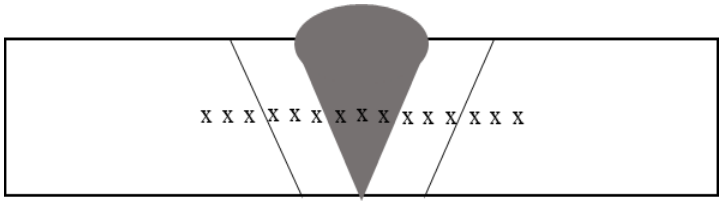

Fig. 4. Indentation points location for hardness test.

3 Results and Discussion

3.1 Macro and Microstructure

Macroscopic images of the cross-sections of the welded joints in the three samples are presented in Fig. 5. It can be seen from Fig. 5 that the width of the HAZ increased with the increase in heat input from 0.52 kJ/mm to 0.92 kJ/mm. Macroscopic images showed the influence of variations in heat input on the size of the HAZ. The distance measured from the fusion line to the BM. Welding using low heat input will have a smaller HAZ size, namely 1.17 mm, for medium heat input the HAZ will be 1.48 mm and for high heat input the HAZ will be larger, namely 2.1 mm. The macroscopic images showed good weld penetration into the BM, and the weld appeared to be free from defects. The welded joints demonstrate that the BM and filler metal have fused properly.

Fig. 6 – Fig. 8 displays the microstructure between the WM and HAZ. Grain growth was expected to be observed in the HAZ bordering the WM. However, the differences in the grain growth or HAZ were not clearly visible under an optical microscope. There was a slight indication that the HAZ of LI had finer grains than those of MI and HI.

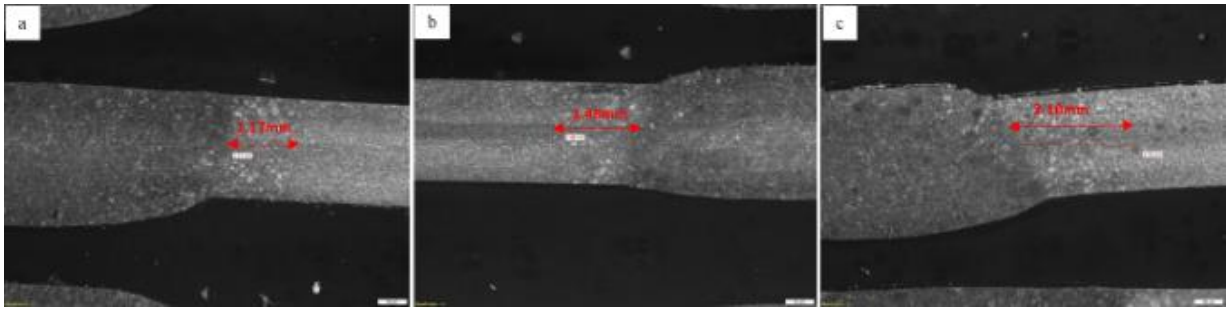

Fig. 5. Macroscopic images of the specimen: a) LI, b) MI, and c) HI.

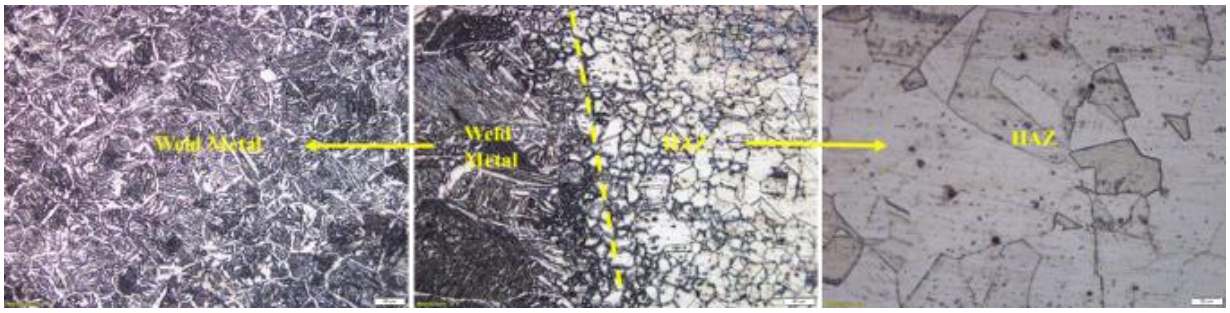

Fig. 6. Microstructure of WM and HAZ in HI specimen with heat input of 924 J/mm.

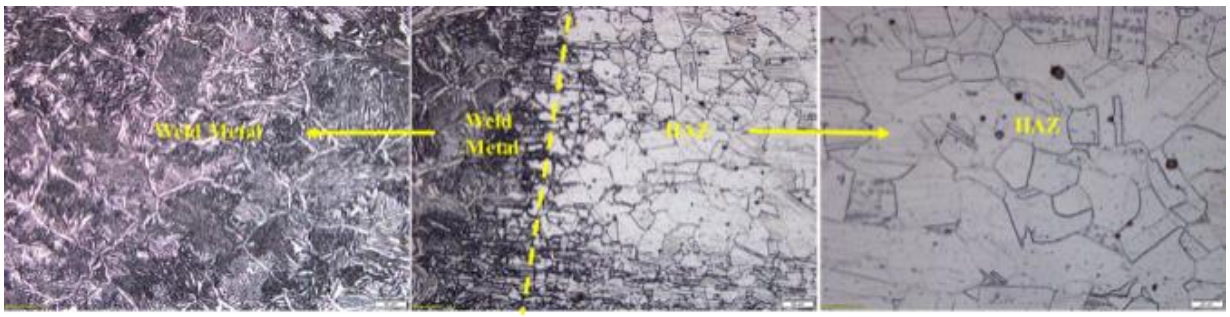

Fig. 7. Microstructure of WM and HAZ in MI specimen with heat input of 635 J/mm.

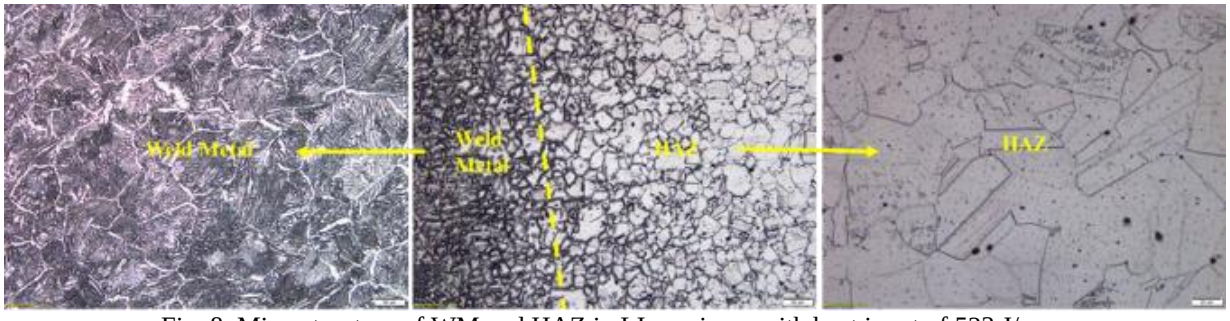

Fig. 8. Microstructure of WM and HAZ in LI specimen with heat input of 523 J/mm.

At higher magnification levels, the microstructure surrounding the fusion line could be observed, as shown in Fig. 9. The observation results indicate the presence of dual structures, namely step structure and ditch structure. The step structure revealed a non-sensitized microstructure, while the ditch structure indicates sensitization [23]. The ditch structure is characterized by a darkening of color at the grain boundaries, indicating the presence of chromium carbide ($Cr_{23}C_6$) precipitates at the grain boundaries. This occurs because chromium migrates to the grain boundaries, resulting in chromium-depleted regions on both sides of the grain boundaries.

Fig. 10 shows the observation results in the HAZ region of the LI, MI, and HI samples. In all three samples, only the step structure was observed. No ditch structure was found in the samples with the variations in heat input. This indicates that the grain boundaries were effectively non-sensitized.

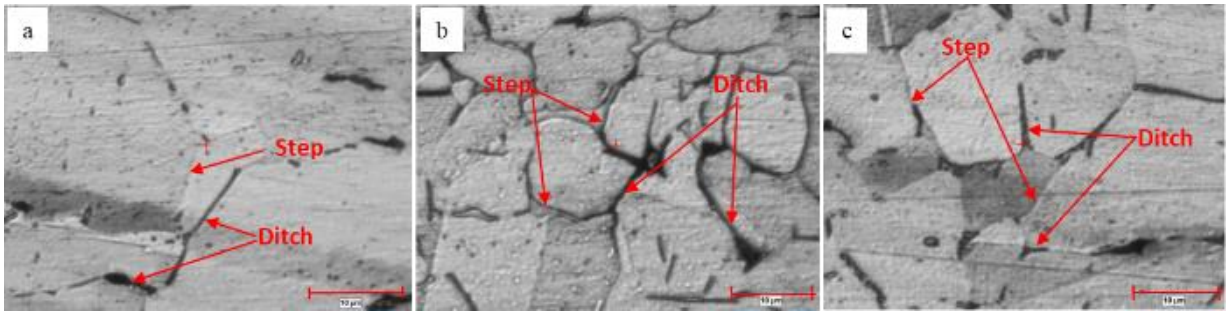

Fig. 9. Microstructure around the fusion line in: a) LI, b) MI, and c) HI.

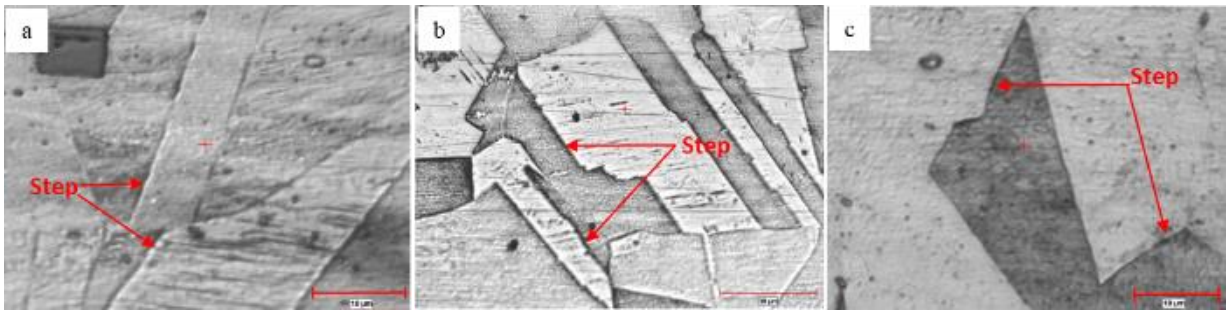

Fig. 10. Microstructure in HAZ of specimens: a) LI, b) MI, and c) HI.

The absence of ditches in the HAZ (Fig. 10) indicated the absence of chromium carbide precipitation at the grain boundaries. The presence of ditches indicates intergranular corrosion. Chromium carbide precipitation was characterised by darker grain boundaries.

3.2 Mechanical Properties

The mechanical tests conducted included tensile testing and hardness testing. The aim was to assess whether performing the welded joints met the standard requirements. The results of tensile strength tests performed at room temperature are presented in Table 4. All nine tensile specimens from the three heat input variations fractured in the base metal (parent metal) as shown in Fig. 11. Thus, it can be concluded that the welded joints were sufficiently strong. This can be attributed to the fact that the tensile strength of the filler metal is higher than that of BM, as shown in Table 2. The welded joints of AISI 321 stainless steel using ER 347 filler metal meet the requirements where the fracture occurs in the base metal (BM) rather than the weld joint. Based on the results, it can be noted that the tensile strength of all welded samples is relatively similar, ranging from 553 to 559 MPa. The average tensile strength of the samples welded with low heat input (LI) was 557 MPa. The average tensile strength of the samples welded with medium heat input (MI) and high heat input (HI) were 555.3 MPa and 555.7 MPa, respectively.

Table 4. Tensile strength results of the welded joint

Test specimen	Tensile strength (MPa)	Elongation (%)	Broken area
LI #1	553	51	BM
LI #2	559	52	BM
LI #3	559	56	BM
MI #1	555	58	BM
MI #2	558	55	BM
MI #3	553	56	BM
HI #1	558	53	BM
HI #2	555	52	BM
HI #3	554	59	BM

The hardness was measured at 15 different mid-depth locations in the WM, HAZ, and BM. Fig. 12 illustrates the results, which showed that the WM and HAZ were harder than the BM. Given its greater carbon content and the alloying elements that the filler metal started, it is possible that the WM had the highest hardness. Because of the chromium carbide growth and faster cooling rate, the higher hardness value in the WM can be linked to a finer microstructure. Microstructure and chemical composition impact the hardness of the WM and HAZ.

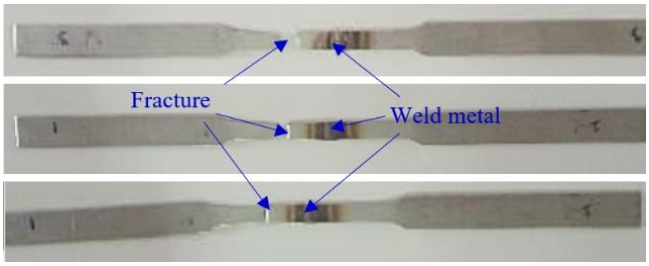

Fig. 11. Tensile specimens for measurement of mechanical properties.

Fig. 12 demonstrates the variation in heat input affects the hardness values in the HAZ and WM region. Welded sample with high heat input (HI) has lower hardness values compared to those with medium (MI) and low heat input (LI). A higher heat input results in a slower cooling rate, increased grain growth, and reduced hardness.

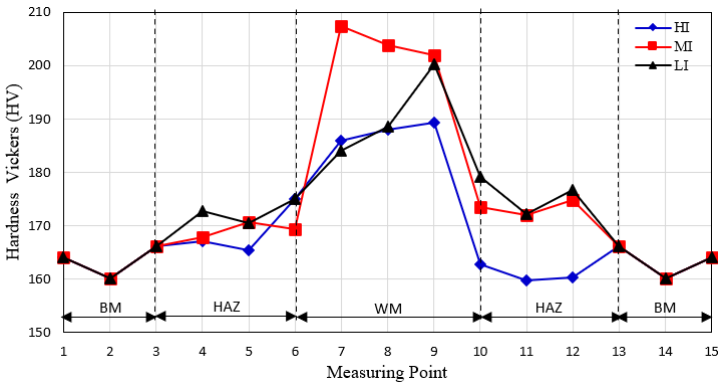

Fig. 12. Hardness measurement results for HI, MI, and LI specimens.

4 Conclusion

The welded joints of AISI 321 stainless steel using ER 347 filler metal exhibit satisfactory performance. The tensile test results showed that fracture occurred in the Base Metal (BM) rather than the weld joint, indicating that the strength of the joint

is higher than that of the BM. It meets the requirements for practical applications.

Welding experiment results show that using three variations of heat input (0.52, 0.64, and 0.92 kJ/mm), it has been demonstrated that higher heat input decreased the hardness of the weld joint. The Weld Metal (WM) had the highest hardness, according to the microhardness test results, followed by the Heat-Affected Zone (HAZ) and BM. This can be attributed to the alloying elements induced by the filler metal, which enhance the hardness of WM.

The microstructural features around the fusion line exhibit both step and ditch structures. The ditch structure indicates intergranular corrosion at the grain boundaries. This differs from the microstructure in the HAZ, which indicates step structures without ditches, indicating no chromium carbide precipitation at the grain boundaries.

References

[1] R. Kriswarini and D. Anggraini, "Studi sensitasi baja tahan karat tipe 316 sebagai bahan kelongsong dan struktur fast breeder reactors," *J. Teknol. Bahan Nukl.*, vol. 11, no. 1, 2016.

[2] A. Setiawan, P. Pribadhi, and M. Ari, "Analisis Pengaruh Heat Treatment terhadap Sifat Mekanik dan Ketahanan Korosi Intergranular SA-240 TP316L," *JST (Jurnal Sains Ter.*, vol. 6, no. 1, pp. 53–59, 2020.

[3] S. Kou, "Welding metallurgy," *New Jersey, USA*, pp. 431–446, 2003.

[4] G. Priyotomo, "Perilaku Sensitasi Pada Logam Stainless Steel Seri J4 Akibat Perlakuan Panas," *Widyariset*, vol. 4, no. 2, pp. 123–132, 2018.

[5] A. Budianto, K. Purwantini, and B. A. T. Sujitno, "Pengamatan Struktur Mikro pada Korosi antar Butir dari Material Baja Tahan Karat Austenitik setelah Mengalami Proses Pemanasan," in *Jurnal Forum Nuklir*, 2009, vol. 3, no. 2, pp. 107–130.

[6] R. Unnikrishnan *et al.*, "Effect of heat input on the microstructure, residual stresses and corrosion resistance of 304L austenitic stainless steel weldments," *Mater. Charact.*, vol. 93, pp. 10–23, 2014.

[7] S. Nishanth, S. Prem, T. Prakash, J. Siva, M. Sathish Kumar, and N. Siva Shanmugam, "Performance Study of Dissimilar Alloy Joints of SS321 and SS347 Under MIG Welding Process," *Trends Manuf. Eng. Manag. Sel. Proc. ICMechD 2019*, pp. 663–671, 2021.

[8] D. Malhotra and A. S. Shahi, "Weld metal composition and aging influence on metallurgical, corrosion and fatigue crack growth behavior of austenitic stainless steel welds," *Mater. Res. Express*, vol. 6, no. 10, p. 106555, 2019.

[9] A. Pardo, M. C. Merino, A. E. Coy, F. Viejo, M. Carboneras, and R. Arrabal, "Influence of Ti, C and N concentration on the intergranular corrosion behaviour of AISI 316Ti and 321 stainless steels," *Acta Mater.*, vol. 55, no. 7, pp. 2239–2251, 2007.

[10] S. M. Kumar and N. S. Shanmugam, "Studies on the weldability, mechanical properties and microstructural characterization of activated flux TIG welding of AISI 321 austenitic stainless steel," *Mater. Res. Express*, vol. 5, no. 10, p. 106524, 2018.

[11] D. Malhotra and A. S. Shahi, "Understanding the role of Ti addition on the corrosion and passive film characteristics of Nb stabilized AISI 347 weld," *Mater. Corros.*, vol. 73, no. 10, pp. 1701–1716, 2022.

[12] H. Oktadinata and A. G. Putra, "Microstructure and Hardness Profile of Dissimilar Lap Joint of Type 304 Stainless Steel to SS400 Carbon Steel," *Met. Indones.*, vol. 41, no. 2, pp. 46–53, 2019.

[13] V. Kumar, H. Arora, P. K. Pandey, and V. Rathore, "Analysis of sensitization of austenitic stainless steel by different welding processes: a review," *Int J Appl Eng Res*, vol. 10, no. 7, p. 1783717848, 2015.

[14] A. D. Fitrianto and R. D. Widodo, "Pengaruh Jenis Filler Terhadap Nilai Kekerasan Dan Struktur Mikro Stainless Steel Aisi 304 Pada Proses Pengerjaan Las Tig," *J. Kompetensi Tek.*, vol. 12, no. 2, 2020.

[15] H. Oktadinata, T. Triantoro, A. Gumilar, and U. R. Jatmiko, "Microstructure and Hardness Properties of AISI 321 Stainless Steel Welded Joints with Different Filler Metal," *Key Eng. Mater.*, vol. 951, pp. 3–9, 2023.

[16] S. K. Gupta, A. P. Patil, R. C. Rathod, V. Tandon, and H. Vashishtha, "Investigation on Impact of Heat Input on Microstructural, Mechanical, and Intergranular Corrosion Properties of Gas Tungsten Arc-Welded Ti-Stabilized 439 Ferritic Stainless Steel," *J. Mater. Eng. Perform.*, vol. 31, no. 5, pp. 4084–4097, 2022.

[17] S. Kumar and A. S. Shahi, "Effect of heat input on the microstructure and mechanical properties of gas tungsten arc welded AISI 304 stainless steel joints," *Mater. Des.*, vol. 32, no. 6, pp. 3617–3623, 2011.

[18] V. A. Setyowati and S. Suheni, "Variasi Arus Dan Sudut Pengelasan Pada Material Austenitic Stainless Steel 304 Terhadap Kekuatan Tarik Dan Strukturmakro," *J. IPTEK*, vol. 20, no. 2, pp. 29–36, 2016.

[19] S. Saravanan, N. Sivagurumanikandan, and K. Raghukandan, "Effect of heat input on microstructure and mechanical properties of Nd: YAG laser welded super duplex stainless steel-Numerical and experimental approach," *Optik (Stuttg).*, vol. 185, pp. 447–455, 2019.

[20] H. Oktadinata, M. Martijanti, P. Ndaruhadi, and E. A. Alsayed, "Study of Sensitization in Gas Tungsten Arc Welded 304 Stainless Steel Joints Using 308L Filler Metal," *Constr. Technol. Archit.*, vol. 11, pp. 3–9, 2024.

[21] M. Kumar, A. Babbar, A. Sharma, and A. S. Shahi, "Effect of post weld thermal aging (PWTA) sensitization on micro-hardness and corrosion behavior of AISI 304 weld joints," in *Journal of Physics: Conference Series*, 2019, vol. 1240, no. 1, p. 12078.

[22] S. Kumar, A. S. Shahi, V. Sharma, and D. Malhotra, "Effect of welding heat input and post-weld thermal aging on the sensitization and pitting corrosion behavior of AISI 304L stainless steel butt welds," *J. Mater. Eng. Perform.*, vol. 30, pp. 1619–1640, 2021.

[23] ASTM International, "Standard Practices for Detecting Susceptibility to Intergranular Attack in Austenitic Stainless Steels," *ASTM A262*, no. September, pp. 1–20, 2015, doi: 10.1520/A0262-15.